

ENHANCED DIELECTRIC CONSTANT AND IMPEDANCE OF PVDF DUE TO INCORPORATION OF PZT IN ITS MATRIX

S. K. PRADHAN^{a*}, A. KUMAR^b, A. N. SINHA^b, P. KOUR^c, R. PANDEY^d,
P. KUMAR^e, M. KAR^d

^aDepartment of Mechanical Engineering, BIT Mesra, Patna Campus, Patna - 800014, India

^bDepartment of Mechanical Engineering, National Institute of Technology, Patna - 800005, India

^cDepartment of Applied Physics, BIT Mesra, Patna Campus, Patna - 800014, India

^dDepartment of Physics, Indian Institute of Technology, Patna, Patna - 801103, India

^eDepartment of Physics, Mahatma Gandhi Central University, Bihar- 845401, India

The Solvent casting method was used to prepare poly(vinylidene fluoride) /lead zirconate titanate i.e.(1-x)PVDF - (x)PZT with $x = 0.00, 0.02, 0.04, 0.06, 0.08$ and 0.10 composites. Dielectric constant of (1-x) PVDF- (x) PZT composites increases with the increase in PZT concentration and is maximum for 4 mole%. Dielectric loss decreases with the increase in PZT concentration in the sample and, it is minimum at 4 mole% PZT. The *ac* conductivity of the sample follows the Jhonscher power law. Impedance analysis indicates both grain and grain boundaries contribution to the conductivity of the sample.

(Received November 19, 2016; Accepted February 10, 2017)

Keywords: Composite, Dielectric constant, Dielectric loss, Impedance

1. Introduction

The material used in hydrostatic sensor, actuators, mechanical sensor, etc. should have good mechanical properties such as hardness, flexibility, high breakdown strength and good electrical properties such as dielectric, piezoelectric properties etc. Polymeric materials show good mechanical properties whereas ceramics show good electrical properties. Composite of ceramics and polymer has these mechanical and electrical properties. In these composites, the polymers are used as matrix and ceramics as the filler or vice-versa. Composites are lighter as compared to ceramics & show 100 times more piezoelectric strain coefficient as compared to that of ceramics [1]. Among the ferroelectric polymer, the best used one is the semicrystalline i.e. half crystalline and half amorphous poly (vinylidene fluoride) PVDF. It is flexible and has mechanical strength which allows making it in different shapes & structures [1- 4]. $\text{CH}_2\text{-CF}_2$ is the monomer unit of PVDF. α , β , γ and δ are the four crystal polymorphs, which are usually present in the crystalline regions [5-6]. TGTG (T-trans G-gauche) conformation, structure was obtained in the nonpolar α – phase [7]. The TTTT planar transformation structure was present in the polar β - phase [7] and TTTGTTTG structure in the γ –phase [8]. The polar β - phase is responsible for the dielectric properties of PVDF. So, filler to be used to make the composite with PVDF as matrix should have a polar structure to enhance the β - phase of PVDF. The most used piezoelectric fillers are lead zirconate titanate (PZT). The composite shows good dielectric, ferroelectric & piezoelectric properties [9-13].

PZT ($\text{PbZr}_{1-x}\text{Ti}_x\text{O}_3$) materials exhibit the most promising piezoelectric property at its MPB (Morphotropic Phase Boundary) which is the 52/48 ratio of Zr/Ti [9]. At this composition, it exhibits both rhombohedral and tetragonal structures. As it is a ceramic material, its brittleness is very high which restricts its applications in mechanical devices. Hence, a composite of PVDF-PZT

*Corresponding author: sudiptabitpatna@gmail.com

are studied to overcome the lacking electrical properties of PVDF and the brittleness of PZT. Mostly the 0-3 connectivity composite has been studied by the researchers [14-26]. Since this connectivity is easy to prepare in the point of commercialization and shows the uniform distribution of PZT filler in the PVDF composites, hence exhibit reproducible physical properties. With the optimized process conditions, structural & material properties of composites with different volume fraction of PZT in PVDF are studied. Dielectric constant of PVDF is very small in comparison to PZT [27-29]. Enriched β phase in PVDF increases the dielectric constant and piezoelectric properties of PVDF – PZT composite [30-34]. The increase in PZT concentration in PVDF increases its electrical properties [35] tensile modulus and degree of crystallinity enhances the piezoelectric properties of PVDF – PZT composite [36-38]. Dielectric and ferroelectric properties of composites increases due to the addition of polar PZT in PVDF matrix [39]. Thermal processing conditions affect the crystalline phase of PVDF which affects its material properties [40-43]. The properties of composites can be used for specific requirements depending on volume fraction, connectivity and properties of constituent phases.

There is still a lack of detail study of dielectric properties of these composite which restricts its wide technological applications. So, the dielectric property of PVDF- PZT at different PZT composition has been studied. The mechanism of dielectric properties has been explained by considering the structure of the material.

2. Experimental

PZT has been prepared by the sol-gel method. 2-methoxy ethanol, acetyl acetone was used as the solvent. Lead (II) acetate trihydrate, zirconium (IV) isopropoxide, titanium (IV) isopropoxide and nitric acid were used as the starting materials. PVDF-PZT composite thick films were prepared by the solvent casting method. The required amount of PVDF was dissolved in DMF (dimethyl formamide). PZT powder was dispersed thoroughly into the solution and was stirred for 6 hours at 50°C and further sonicated for 50 minutes at this temperature. The prepared solution was cast into a petri dish & heated at 100°C for 24 hours to get the desired film. The process was repeated with other different weight fraction (2-10% of PZT). Field emission scanning electron microscopy (FESEM, JEOL) was used to study the surface morphology of the film. To measure the dielectric and impedance properties of the sample N4L LCR meter (PSM 1735) was used. The dielectric measurement was carried out in the frequency range of 10^2 - 10^6 Hz and temperature range of 40-120 °C.

3. Result and Discussion

Fig.1(a- e) shows FESEM micrographs of PVDF-PZT composite thick films. It indicates that system is homogenous without wrinkles, cracks & deformation. (1-x) PVDF - (x) PZT system with $x = 0.04$ shows prominent grains with grain boundaries. (1-x) PVDF - (x) PZT system with $x = 0.8$ and 0.10 shows small grains with grain boundaries. The PVDF grains are in μm range.

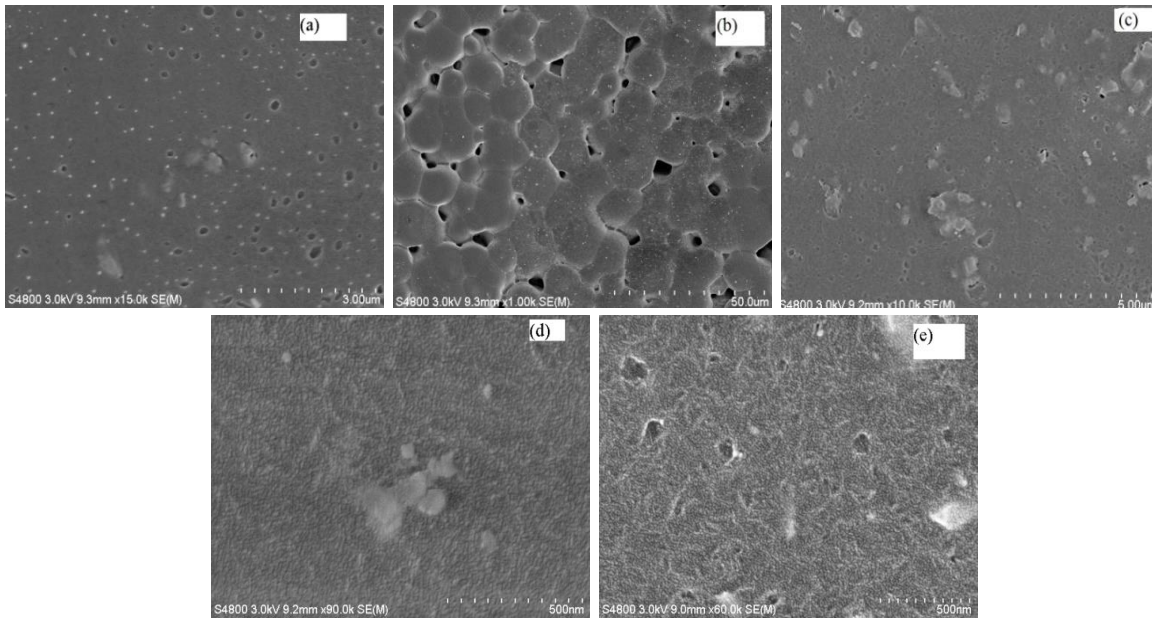


Fig. 1. FESEM micrographs of, (1-x) PVDF - (x) PZT system for (a) $x = 0.02$, (b) $x = 0.04$, (c) $x = 0.06$, (d) $x = 0.08$, and (e) $x = 0.1$ samples.

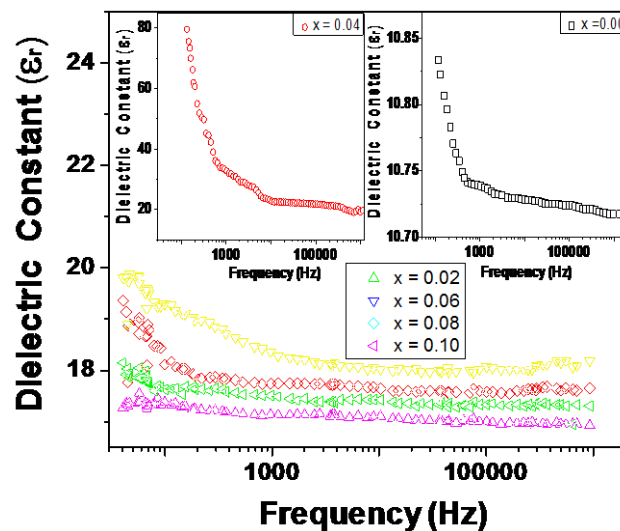


Fig.2. Variation of Dielectric constant with frequency of (1-x) PVDF - (x) PZT system for $x = 0.00, 0.02, 0.04, 0.06, 0.08$ and 0.10 samples. Inset shows for $x = 0.00$ and 0.04 for the clarity as their dielectric constant is lowest and highest respectively.

Variation of frequency dependent dielectric constant of (1-x) PVDF - (x) PZT composite for $x = 0.00 - 0.10$ shown in fig.2. Dielectric curve follows the usual nature of dielectric material. At the low frequency dielectric constant was higher and it decreases with the increase in frequency. The dielectric constant decreases with the increase in frequency for all the composition of (1-x) PVDF - (x) PZT. The dielectric constant is maximum at low frequency due to contribution from different types of polarizations such as ionic, electronic, dipole and space charges. The dielectric constant decreases with increase in frequency is possibly due to the easy depolarization of dipoles that exist in weak bonded interface & boundary regions. So, orientational polarization is the main factor which restricts the dielectric constant at higher frequencies. Dielectric constant of PVDF increase with increase in PZT concentration in the sample up to 4%. The dielectric constant decreases with the increase in PZT concentration for more than 4%

of the sample. The increase in dielectric constant up to 4% of PZT in the composite are attributed to the lattice strain in the composite. This lattice strain is introduced in the sample with the incorporation of PZT in the composite. The incorporated PZT with MPB composition having a rhombohedral and the tetragonal structure reported earlier [44-45]. But these structures undergoes compression and elongation at PZT and PVDF interface. It introduced lattice strain in the sample. The lattice strain decreases with the increase PZT concentration in the sample result in decrease dielectric constant of the sample. The dielectric constant of PVDF-PZT composite increases as compared to the pure PVDF. XRD, Raman and FTIR study show the presence of α , β and γ phase in the composite reported elsewhere. α and γ phase show nonpolar structure. So their net dipole moment is zero and hence the electric polarization in the composite is hindered by this polymeric chain. As a result the dielectric constant of composite is lowered as compared to pure PZT [47]. But the β phase represents the polar structure i.e in β phase H and F in the C-F and C-H bond are in the same chain and perpendicular to the carbon [48]. So has a net dipole moment and the net dipole moment per unit cell increases due to these β phase in the sample. 4 mole% of PZT in PVDF-PZT composition shows the maximum contribution from β phase, which shows maximum dielectric constant as compared to others [46].

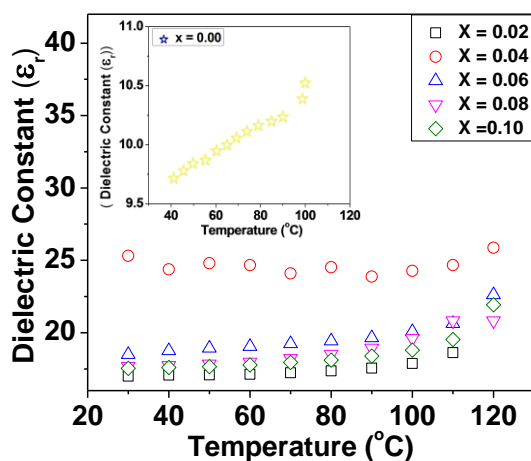


Fig.3. Variation of Dielectric constant with temperature of (1-x) PVDF - (x) PZT system with $x = 0.00 - 0.10$ samples

Fig.3. Shows the variations of dielectric constant with temperature for (1-x) PVDF - (x) PZT composite system with $x = 0.00 - 0.10$. The dielectric constant increases with the increase in temperature. At higher temperature, the dielectric constant increases more rapidly as compared to that at lower temperature. At higher temperature, the polar group is aligned due to the breakup of the polymeric chain, resulting higher the dielectric constant of the composite. Maximum dielectric constant at elevated temperature was also obtained for (0.96) PVDF-(0.04) PZT composite. It is due to the presence of more prominent β -phase of PVDF and the lattice strain of the structural asymmetry in PZT.

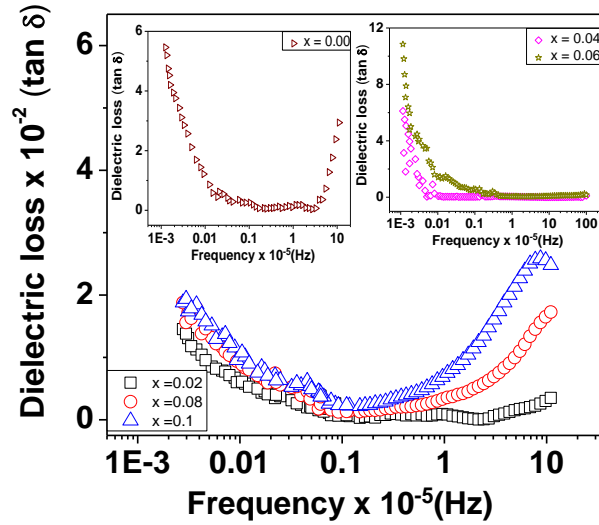


Fig.4. Variation of Dielectric tangent loss ($\tan\delta$) with frequency of (1-x) PVDF - (x) PZT system with (a) $x = 0.02$, (b) $x = 0.04$, (c) $x = 0.06$, (d) $x = 0.08$, and (e) $x = 0.1$ samples. Inset shows for $x = 0.00$ and 0.04 for the clarity as their dielectric loss is highest and lowest respectively

Fig.4 shows the variation of dielectric loss with a frequency of (1-x) PVDF - (x) PZT composite system with $x = 0.00 - 0.10$. The dielectric loss of the composite was decreased with the increase in frequency of the sample up to 10 kHz. The dielectric loss increases with the further increase in frequency since the dipoles are not able to follow the oscillating field. (0.96) PVDF-(0.04) PZT composite shows the small dielectric loss as compared to the other composition of (1-x) PVDF - (x) PZT system.

The conductivity of the composite was calculated by using the equation;

$$\sigma_{ac} = 2\pi f \epsilon_0 \epsilon_r \tan\delta \quad (3)$$

Where f is the frequency, $\tan\delta$ (loss) is the dissipation factor, ϵ_0 & ϵ_r are the permittivity of free space and relative permittivity of the sample respectively. The frequency dependent ac conductivity of (1-x) PVDF - (x) PZT system with $x = 0.00 - 0.10$ composite has been depicted in the above fig.5. The ac conductivity of the sample increases with the increase in PZT-PVDF composite up to 4 mole% and then it decreases. The low frequency range conductivity corresponds to the dc conductivity of the sample. The diffusion of randomly spread ionic charge carriers through activated hopping gives rise to the dc conductivity of the composites. At high frequency dispersion was observed in the graph. The data points of ac conductivity were analyzed by the Jonscher's power law, which defined as,

$$\sigma(\omega) = \sigma_0 + A\omega^n \quad (4)$$

Where σ_0 is the frequency independent conductivity, A is the temperature dependent pre exponential factor and n is the frequency exponent. The value of n lies in between 0 to 1. These n values are compared to those reported by other groups [50-51]. The frequency exponent n represents the degree of interaction between the mobile ions with the lattices [52- 54]. When the interactions between neighboring dipoles are almost negligible the value of n is one. The A and n values of (1-x) PVDF-(x) PZT system for $x = 0.00 - 0.10$ are enlisted in the table 2. The value of n decreases with the increase in PVDF percentage in PZT- PVDF composite up to $x = 0.04$ and increases with further increase of PVDF. The increase of lattice strain with the increase of PZT due to structural change causes the decrease of mobile ions and lattice strain. Hence, the value of n decreases with increase in PZT and have a minimum value of 4 mole% of PZT. The value of A increases with the increase of PVDF concentration in PZT - PVDF composite and has a maximum value of $x = 0.04$. A represent the ferroelectric properties of the sample. The maximum lattice strain at 4mole% of the

PZT also reflected on the value of A. So conductivity analysis also shows that the dielectric properties were maximum at $x = 0.04$ concentrations of the PZT due to lattice strain

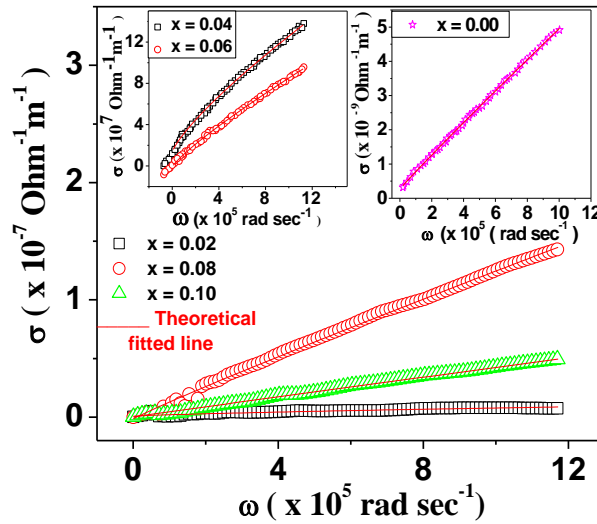


Fig.5. Variation of ac conductivity with frequency spectra of $(1-x)$ PVDF - (x) PZT composite system with $x = 0.00 - 0.10$

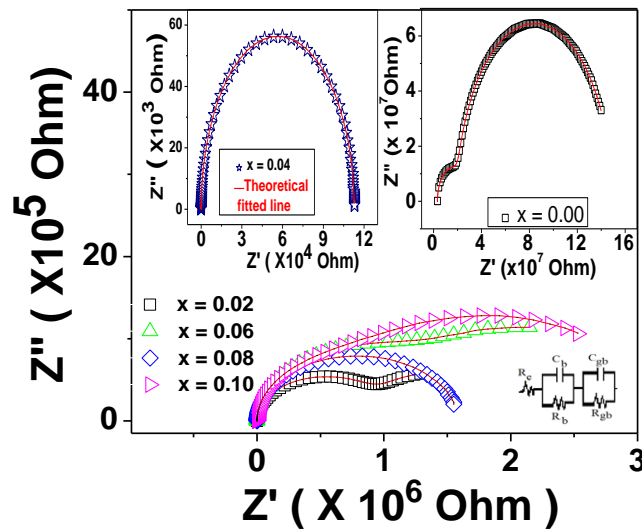


Fig. 6 Cole Cole plot of $(1-x)$ PVDF - (x) PZT composite for (a) $x = 0.00$, (b) $x = 0.02$, (c) $x = 0.04$ (d) $x = 0.06$, (e) $x = 0.08$, and (f) $x = 0.10$ samples.

To get a detailed picture of the electrical properties of PVDF-PZT composite, the complex impedance spectroscopy technique is used [55]. In frequency domain, the contribution of various components such as grain, grain boundary and electrode interface to the electrical resistivity is calculated. Four basic ways are used to represent the data points in the complex plane such as complex impedance (Z^*), complex electric modulus (M^*), complex admittance (Y^*) and complex permittivity (ϵ^*) to represent the data points in the complex plane. Complex impedance (Z^*) data points are used to plot the Cole Cole curve of $(1-x)$ PVDF- (x) PZT composite for (a) $x = 0.00$, (b) $x = 0.02$, (c) $x = 0.04$, (d) $x = 0.06$, (e) $x = 0.08$, and (f) $x = 0.10$ are shown in the Fig. 6. Complex impedance Z^* is represented as $Z^* = Z' - j Z''$, where Z' is the real part of the impedance, Z'' represent the imaginary part of impedance, $\omega = 2\pi f$ is the angular frequency, $j = \sqrt{-1}$ is the imaginary factor. To explain the complex impedance of electrode/sample/electrode, the data points are fitted

with different equivalent electric circuit. ZSimpWin software was used to fit the equivalent parallel resistance and capacitance circuit to the data points. The data points are represented by the symbol and the fitted circuit by the broad line. The data points show two semicircular loops. So $R_e(R_gC_g)(R_{gb}C_{gb})$ was used to analyze the data points. R_e represents the resistance due to the electrode, R_g represents the resistance due to the grain, R_{gb} represents the resistance due to the grain boundary, C_g represents the capacitance due to grain and C_{gb} represents the capacitance due to grain boundaries. The semicircular arc at low frequency represent contributions from grain boundary, whereas the contribution of grain was represented by an arc at high frequency. For pure PVDF the contribution of grain is more in comparison to grain boundary. The contribution from grain boundary decreases whereas the contribution from grain increases with the increase in PZT concentration in PVDF. At 4mole % of PZT the contribution of grain is more as compared to the grain boundary. The FESEM micrograph also clearly shows the result and dielectric behavior also maximum at this composition. Above 4mole% the grain boundary resistance increases and grain increases.

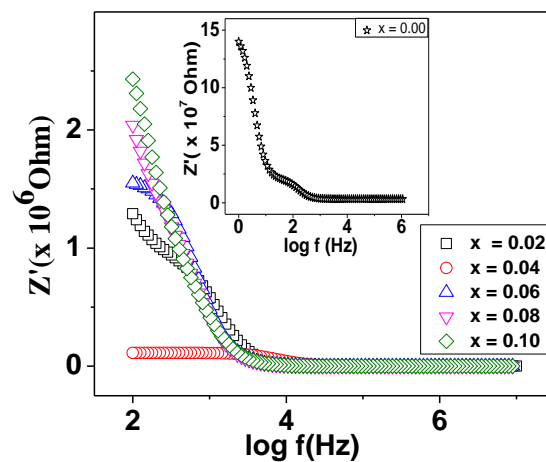


Fig. 7. Real part of impedance (Z') versus frequency of (1-x) PVDF-(x) PZT system with $x = 0.02, 0.04, 0.06, 0.08$ and 0.10

Figure 7 shows the variation of the real part of impedance (Z') with frequency of (1-x) PVDF-(x) PZT system for $x = 0.02 - 0.10$. It was observed that the magnitude of Z' was decreased with increase in frequency up to 10k Hz. Z' values merge after 10 kHz frequency due to release of space charges [56-57].

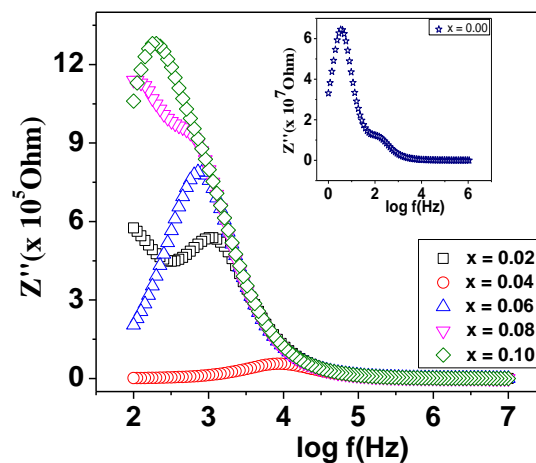


Fig.8. Imaginary part of impedance (Z'') versus frequency of (1-x) PVDF-(x) PZT system for $x = 0.02 - 0.10$

Fig. 8. depicts the variation of the imaginary part of impedance (Z'') with frequency of (1-x) PVDF-(x) PZT system with $x = 0.02 - 0.10$. The curves show that the Z'' value increases with the increase in frequency and reaches to a maximum (Z''_{max}) at a particular frequency and then decreases. The value of Z''_{max} shifts to a higher frequency with the increase in PZT concentration in PVDF-PZT composites. Maximum shift in Z''_{max} is obtained at the 4mole% of PZT in PVDF-PZT composite. Z''_{max} shifts to lower frequency with the further increase in PZT concentration in PVDF-PZT composites. The appearance of peak in the curve shows relaxation in the system. The FWHM (full width at half maximum) is large at 4 mole % of PZT in PVDF. The relaxation is large for 4 mole% of PZT. So the dielectric property is maximum at this composition. The peak analysis shows that it is symmetric, hence it shows the Debye type relaxation behavior [58].

4. Conclusions

(1-x) PVDF-(x) PZT composite has been studied for the composite $x = 0-0.10$. Dielectric constant increases with the increase in PZT concentration and, it was maximum at $x = 0.04$ concentrations of PZT in the composite. Dielectric loss decreases with the increase in PZT concentration in PVDF. Dielectric loss was a minimum for 4 mole% of PZT in PVDF-PZT composite. Ac conductivity follows the Johnson power law. Impedance analysis shows the contribution from both grain and grain boundaries. The present study indicates the possible application of 4 mole% PVDF-PZT composite for the dielectric applications.

References

- [1] M. Sharma, G. Madras, S. Bose, *Phys Chem Chem Phys* **16**, 16492 (2014).
- [2] M. Sharma, G. Madras, S. Bose, *Phys Chem Chem Phys* **16**, 14792 (2014).
- [3] H.J. Ye, L. Yang, W. Z. Shao, S. B. Sun, L. Zhen, *RSC Adv* **32**, 3730 (2013).
- [4] S. Satapathy, S. Pawar, P. K. Gupta, K. B. R. Varma, *Bull. Mater Sci* **34**, 727 (2011).
- [5] A. J. Lovinger, *Macromolecules* **14**, 322 (1981).
- [6] J. B. Lando, H. G. Olf, A. Peterlin, *J Polym Sci Part A* **4**, 941 (1966).
- [7] A. Lovinger, *In developments in crystalline polymer*, edited by D. C. Bassett. Applied science Publishers Ltd, N.J. Englewood (1982).
- [8] A. K. Koray, E. dogan, M. Allahverdi, A. Safari, *Ferroelectrics* **52**, 746 (2005).
- [9] B. Jaffe, W. R. Cook Jr, H. Jaffe, *Piezoelectric ceramics*, Academic press, London, UK (1971).
- [10] A. Safari, E. K. Akdogan, *Piezoelectric & Acoustic materials for transducers applications* Springer, New York (2008).
- [11] Z. Ye, *Handbook of advanced dielectric, piezoelectric & ferroelectric materials synthesis, properties & applications*, CRC press, North America (2008).
- [12] R. Guo, L. E. Cross, S. E. Park, B. Noheda, D. E. Cox, G. Shirane, *Phy Rev letter* **84**, 5423 (2000).
- [13] A. G. Khachatryan, *Philos Mag* **90**, 37 (2010).
- [14] K. S. Lam, Y. W. Wong, L. S. Tai, Y. M. Poon, F. G. Shin, *J. Appl. Phys.* **96**, 3896 (2004).
- [15] C. W. Nan, G. J. Weng, *J of Appl Phys* **88**, 416 (2000).
- [16] C. K. Wong, F. G. Shin, *J Appl Phys* **97**, 064111 (2005).
- [17] P. Han, S. Pang, J. Fan, X. Shen, T. Pan, *Sens. Actuators A* **204**, 74 (2013).
- [18] X. D. Chen, D. B. Yang, Y. D. Jiang, Z. M. Wu, D. Li, F. J. Gou, J. D. Yang, *Sens Actuators A* **65**, 194 (1998).
- [19] F. Fang, W. Yang, M. Z. Zhang, Z. Wang, *Sci Technol* **69**, 602 (2009).
- [20] S. Mendes, C. M. Costa, V. Sencadas, J. Nunes, P. Costa, J. R. Gregorio, S. L. Mendes, *Appl Phys A* **96**, 899 (2009).
- [21] H. Chen, X. Dong, T. Zeng, Z. Zhou, H. Yang, *Ceram Int* **33**, 1369 (2007).
- [22] Y. J. Choi, M. J. Yoo, H. W. Kang, H. G. Lee, S. H. Han, S. Nahm, *J Electro Ceram* **30**, 30 (2013).
- [23] Y. M. Poon, C. H. Ho, Y. W. Wong, F. G. Shin, *J Mater Sci* **42**, 6011 (2007).
- [24] Y. H. Son, S. Y. Kwon, S. J. Kim, Y. M. Kim, T. W. Hong, Y. G. Lee, *Integr Ferroelectric*

88,44(2007).

- [25] A. K. Zak, W. C. Gan, W. Majid, H. Darroudi, Velayutham A. M. Ceram. Int **37**, 1653(2011).
- [26] Z. Ahmad, A. Prasad, K. Prasad, PHYSICA B **404**, 3637(2009).
- [27] P. Kim, S. C. Jones, PHotchkiss J. Adv. Mater **19**, 1001(2007).
- [28] K. Uchino, Ferroelectric Devices Marcel Dekker, Basel(2000).
- [29] S. Ahmed, F. R. Jones, J Mater Sci **25**, 4933(1990).
- [30] S. Chen, K. Yao, F. E. H. Tay, C. L. Liow, Applied physics **102**, 104108(2007).
- [31] T. Furukawa, J. Aiba, E. Fukada, J Applied physics **50**, 3615(1979).
- [32] J. Lovinger, T. Furukawa, G. T. Davis, M. G. Broadhurst, Polymer **24**, 1225(1983).
- [33] R. Gregorio, M. Cestari, Fe Bernardino, J. Material Sci **31**, 2925(1996).
- [34] T. Yamada, T. Ueda, T. Kitayama, J Applied physics **53**, 4328(1982).
- [35] B. Hilezer, J. E. Kutek Markiewicz, processing of electroceramics(2003).
- [36] Pailyn Thongsanitgarn, Anucha Watcharapasorn, Sukanda Jiansirisomboon, Surface Review and Letters **17**, 1(2010).
- [37] C. W. Nan, G. J. Weng, J Appl Phys **88**, 416(2000).
- [38] S. F. Mendes, C. M. Costa, V. Sencadas, J. S. Nunes, P. Costa, J. R. Gregorio, S. L. I. Mendes, Appl Phys A **96**, 899(2009).
- [39] P. Gowdhaman, M. Haresh Pandya, P. R. Kumar, V. Annamalai, J Environ Nanotechnol **4**, 28(2015).
- [40] C. J. Dias, D. K. Das-Gupta, IEEE Trans. Diel Elect Ins **7**, 6(1996).
- [41] V. Tiwari, G. Srivastava, J Polym res **21**, 587(2014).
- [42] R. E. Newnham, L. J. Bowen, K. A. Klinker, L. E. Cross, J Mater Eng **2**, 93(1980).
- [43] R. E. Newnham, D. P. Skinner, L. E. Cross, Mater Res Bull **13**, 525(1978).
- [44] D. P. Skinner, R. E. Newnham, L. E. Cross, Mater Res Bull **5**, 997(1978).
- [45] P. Kour, Pawan Kumar, SK Sinha, Manoranjan Kar, Solid State communications **190**, 33(2014).
- [46] P. Kour, Pawan Kumar, S. K. Sinha, Manoranjan Kar, J Mater Sci: Mater Electron **26**, 1304(2015).
- [47] S. Satapathy, S. Pawar, P. K. Gupta, K. B. R. Varma, Bull Mater Sci **34**, 727(2011).
- [48] Y. Bormashenko, Pogerb, R. O. Stanevsky, O. E. Bormashenk, Polym Testing **23**, 791(2004).
- [49] J. Wang, H. Li, J. Liu, Y. Duan, S. Jiang, S. J. Yan, Am Chem Soc **125**, 1496(2003).
- [50] P. Thomas, K. T. Varughese, K. Dwarakanath, K. B. R. Varma, Sci Technol **70**, 539(2010).
- [51] S. Chen, K. Yao, F. E. H. Tay, C. L. Liow, J Appl Phys **102**, 104108(2007).
- [52] A. K. Jonscher, J. Appl. Phys **32**, 57(1999).
- [53] A. K. Jonscher, Dielectric Relaxation in Solids, Chelsea Dielectric Press, London(1983).
- [54] B. Patti, B. C. Sutar, B. N. Parida, P. R. Das, R. N. P. Choudhary, J Material Science Mater Electron **24**, 1608(2013).
- [55] S. Saha, T. P. Sinha, Phys Rev B **65**, 134103(2002).
- [56] C. Leon, A. Rivera, A. Varez, J. Sanz, Santamaria, K. L. Nagi, Phys Rev Lett **86**, 1279(2001).
- [57] J. R. Mac Donald, Impedance spectroscopy, Wiley, New York(1987).
- [58] B. Behera, P. Nayak, R. N. P. Choudhary, Eur J Phys **6**, 289(2008).